Available online at www.sciencedirect.com

ScienceDirect

Procedia Engineering 00 (2017) 000–000

SAND2017-3527C

Procedia Engineering

www.elsevier.com/locate/procedia

14th Hypervelocity Impact Symposium 2017, HVIS2017, 24-28 April 2017, Canterbury, Kent, UK

Eulerian Hydrocode Estimates of Richtmyer-Meshkov Instability Growth and Arrest

S.P. Rojas[a*], E.N. Harstad[b], R.G. Schmitt[b]

[a]*Redtower Labs, P.O. Box 32057, Washington, DC 20007 USA*
[b]*Sandia National Laboratories, P.O. Box 5800, MS0836, Albuquerque NM 87185 USA*

Abstract

Following previous experimental evidence of growth and arrest of Richtmyer-Meshkov instabilities in copper, we have used the CTH shock physics code to study and calibrate the effects of material strength at high strain rates. Highly resolved one and two-dimensional simulations were performed using the Johnson-Cook (JC), Mechanical Threshold Stress (MTS), and Preston-Tonks-Wallace (PTW) strength models. The one-dimensional simulations utilized a prescribed homogeneous deformation strain path covering strain rates observed in previous hydrodynamic instability experiments. Spall was modeled using a nominal threshold pressure model (PFRAC) and we use the Mie-Gruneisen equation of state to estimate the volumetric response of the experiments. Our results show good qualitative and quantitative agreement between numerical estimates and prior experiments in the strain rate regimes of interest.

Peer-review under responsibility of the scientific committee of the 14th Hypervelocity Impact Symposium 2017.

Keywords: Richtmyer-Meshkov instability; material strength; hypervelocity impact

1. Introduction

Material strength plays an important role in many high pressure, high strain rate events such as spacecraft debris shield performance, armor design, and planetary science impact problems. Hypervelocity impact phenomena of interest can reach strain rates exceeding 10^{11} s^{-1} and pressures exceeding 10 GPa [1]. Modeling such phenomena is complicated by the fact that material strength is sensitive to many parameters such as crystal structure, deformation history, and grain size [2]. Both empirically based constitutive models, such as Johnson-Cook [3], as well as more physically based models for plastic flow, such as MTS [4,5] and PTW [6], rely on experimental data within a relatively narrow span of strain rates. For lower rate regimes (10^{-4} to 10^{-1} s^{-1}) mechanical testing machines are used

Peer-review under responsibility of the scientific committee of the 14th Hypervelocity Impact Symposium 2017.

to generate data while for higher strain rates up to 10^4-10^5 s^{-1} split Hopkinson bar (SHB) tests, Taylor anvil tests, and flyer plate experiments have been used to generate families of stress-strain curves for constitutive modeling [7]. Above the so-called "thermal activation" regime of 10^4 s^{-1} validated experimental data is relatively sparse. The work presented here focuses on this intermediate regime of 10^4 – 10^9 s^{-1} by comparing Eulerian hydrocode estimates of Richtmyer-Meshkov instability growth and arrest at strain rates of 10^7 s^{-1} with previous experimental results [8]. Computational results for the entire strain rate span of interest, from thermal activation through overdriven shock above 10^9 s^{-1}, were generated by driving the Johnson Cook, PTW, and MTS constitutive models through a prescribed deformation history.

A Richtmyer-Meshkov instability develops when a plane shock wave collides with a corrugated interface separating two different fluids [9,10]. At the interface, part of the incident shock wave is transmitted, and part is reflected, forming pressure oscillations which alternately place the material in tension and compression [11]. Piriz observed that the interface oscillates harmonically at a rate that depends on the shear modulus [12]. In recent years, RMI experiments have received renewed interest as a means to study material strength at intermediate strain rates because of the relative ease and low cost for performing the experiments [13,14]. Figure 1 shows a basic illustration of the Richtmyer-Meshkov configuration. The "spikes" shown in the illustration experience a pressure gradient which tends to cause the instability to grow, fed by the "bubbles".

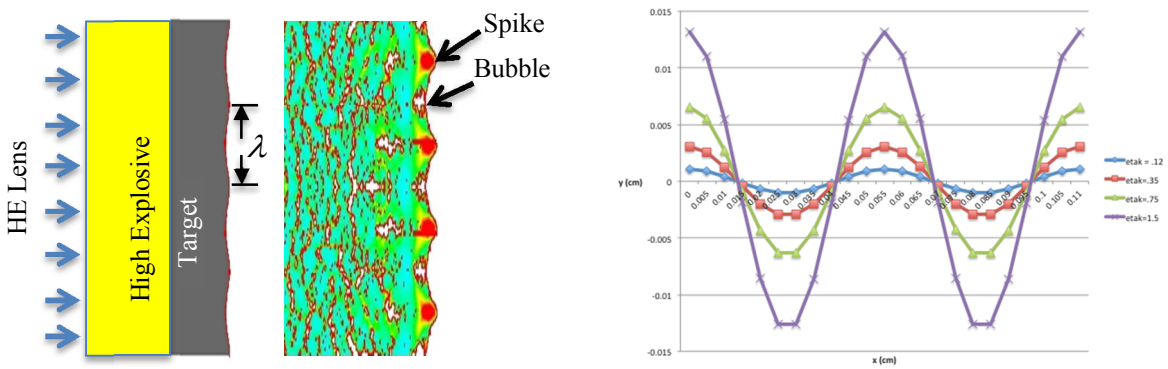

Fig. 1. (a) basic RMI experiment setup (b) various "corrugation" runs that were completed as part of this study

2. Models

2.1. RMI Simulations

Release 11.2 of the CTH shock physics code was used [15] to examine the effects of different strength models on Richtmyer-Meshkov instability formation. CTH estimates were compared to experimental measurements reported in [8]. Baseline simulations focused on the $\eta_0 k = .35$ configuration (Figure 1b) following experimental evidence [8] that arrest and growth occurs with this surface corrugation. Each 2D simulation used 5 μm per cell (providing approximately 5 cells across the width of the perturbation), periodic boundary conditions, and a simple spall model specifying the pressure at which tensile failure occurs. Figure 2 illustrates the basic CTH model setup along with a graphical depiction of how the spike length, η_∞-η_0, was computed using tracer particles positioned at the free surface and spike positions. Uncertainty in computing η_∞-η_0 in this manner was estimated to be roughly ±2μm. The JWL equation of state for PBX-9501 explosive was used and three different strength models for copper were compared: PTW, MTS, and Johnson-Cook. The experiments of interest utilized OFHC half-hard copper with grain sizes on the order of 20 μm [8]. The minimum tensile fracture stress value (PFRAC) used for each simulation was 3 GPa (3 x10^{10} dyne/cm^2).

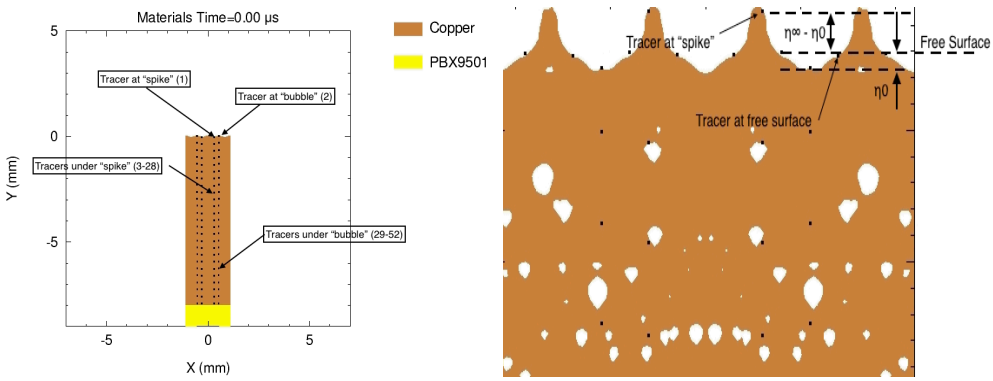

Fig. 2. Illustration of (a) the CTH model with tracer particles and (b) sample results from the Johnson-Cook run.

2.2. Prescribed Deformation Simulations

The prescribed deformation (PRDEF) capability in CTH was used to investigate the MTS, PTW, and Johnson-Cook flow stress models in 1-dimensional uniaxial tension and compression. PRDEF allows users to run their model under a variety of standard and non-standard homogeneous deformations in which every cell experiences identical strains, that are explicitly prescribed in the CTH input file. Thus the PRDEF functionality enables users to test various strength and equation of state models in simple controlled configurations and extreme conditions.

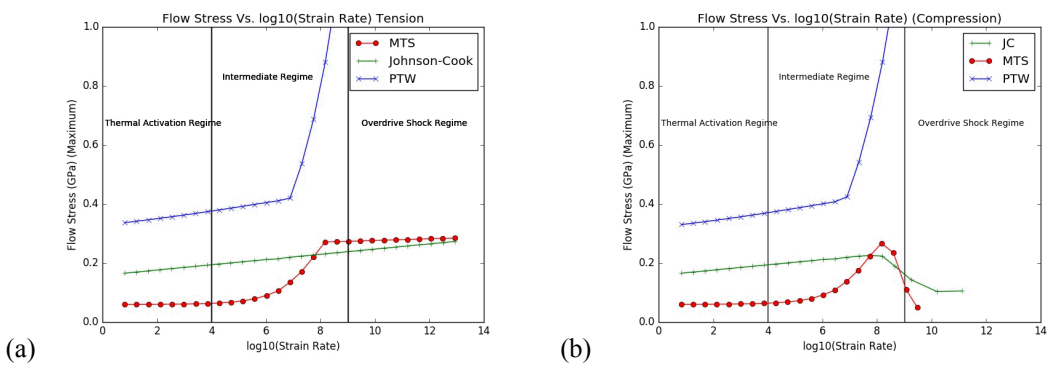

Fig. 3. Plots of Flow Stress vs. log Strain Rate for MTS, PTW, and Johnson-Cook (a) Uniaxial Tension (b) Uniaxial Compression

Using this capability, the compression/rarefaction oscillations seen in the RMI problem were isolated and studied independently without the complex wave interactions in the full problem. Several hundred CTH runs were completed in order to investigate the performance of each model as a function of strain rate. Using prescribed strain paths to obtain strain rates in all three regimes (thermal activation, intermediate, and overdriven shock), stress strain curves were generated for both compression and tension using the strength models of interest (Figure 3).

3. Results

3.1. RMI Simulations

As shown in Table 1 all of the models do a fairly good job of estimating perturbation growth considering that at the strain rate of ~ 10^7 s^{-1} the models are well outside of their experimentally calibrated range. The strength

computed by the Johnson-Cook model as manifested in the perturbation growth is too low compared to value of 160 μm measured by Buttler [8] for the $\eta_0 k = .35$ case. Conversely, the strength computed by the MTS and PTW models is too high compared to the experimental spike height measurement. Peak strain rates for PTW, MTS, and Johnson-Cook were all around 1.4 $x10^7$ to 4.3$x10^7$ s^{-1} (Figure 6) which agrees well with the experimentally measured average value of 1.5$x10^7$ s^{-1}. Peak velocity estimates for each strength model are very close to the experimentally measured value of 2.15 mm/μs suggesting that the JWL equation of state for detonation products and the PTW, MTS, and JC strength models do an adequate job of capturing the initial shock loading of the copper target. The uncertainty in the experimentally measured velocity as reported in [8] was on the order of .01 - .02 mm/μs.

Using the Johnson-Cook model, it was found that the tail of the velocity profile (approximately .5 μs to 2 μs in Figure 5b), could be either steepened to rapid decay or flattened by varying the amount strain rate hardening in the Johnson-Cook model ("C" parameter). Somewhat surprisingly, the amount of strain rate hardening was observed to have a much greater effect on the tail structure than the fracture strength value. Although this trend was also observed when using the more advanced Johnson-Cook fracture model, an in-depth investigation of fracture effects was not pursued since the focus of this study was on material strength modeling.

Table 1. Summary of Baseline CTH Results Compared to Experiment (5 μm mesh)

Strength Model	η_∞-η_0 (μm)	Peak Velocity (mm/μs)
Johnson-Cook (Cu)	245	2.17
PTW(Cu)	103	2.11
MTS (OFHC Cu)	127	2.10
Experiment (1/2 Cu)	**160**	**2.15**

Figure 4 illustrates the variability in strength and resulting plastic strain across each model shortly after the shock wave reaches the free surface (the intermingled red lines are tracer particles for higher resolution under the spike). Interestingly, when the spall bubbles seen in Figure 4 were suppressed by using a very high value for fracture strength, a late time release wave propagated to the free surface causing a second additional increase in plastic strain and spike growth. In this case, no spall layers were formed to disconnect the release wave from the free surface. This highlights the potential value of well diagnosed RMI experiments in improving not only material strength models, but also fracture models.

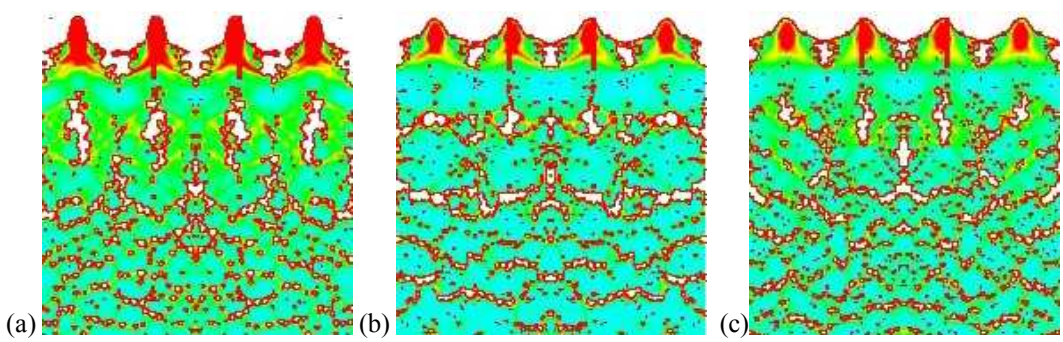

Fig. 4 Plastic Strain at 3.8 μs from shock arrival at the free surface (red = 1.0; green= 0.0) (a) Johnson-Cook (b) MTS (c) PTW

The Mie-Gruneisen equation of state used in the calculations yielded shock release temperatures and pressures at the HE/metal interface of around 784-787 K and 55 GPa for all models, suggesting that the material is not melted on initial shock. All strength models indicated that shock heating and adiabatic heating due to plastic work are not high

enough to melt the material. Figure 5a shows a plot of flow stress as a function of time for the tracer particle placed at the spike tip. The time averaged spike flow stress for PTW, JC, and MTS respectively was .26 GPa, .19 GPa, and .38 GPa.

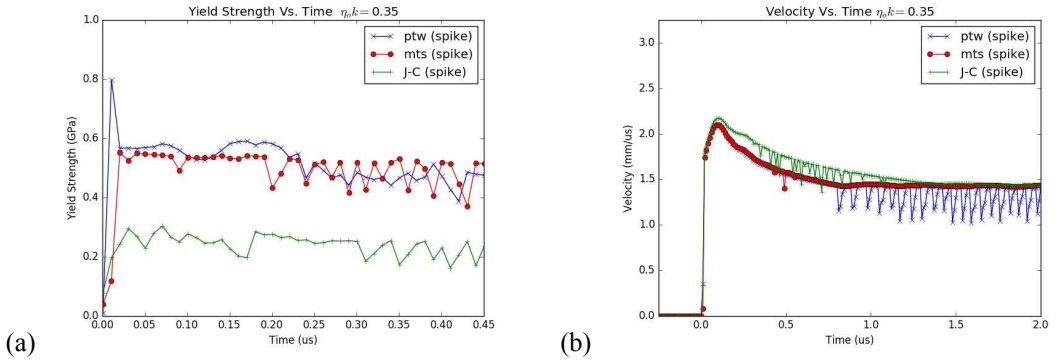

Fig. 5 Results for the RMI simulation for each model (a) yield strength and (b) velocity.

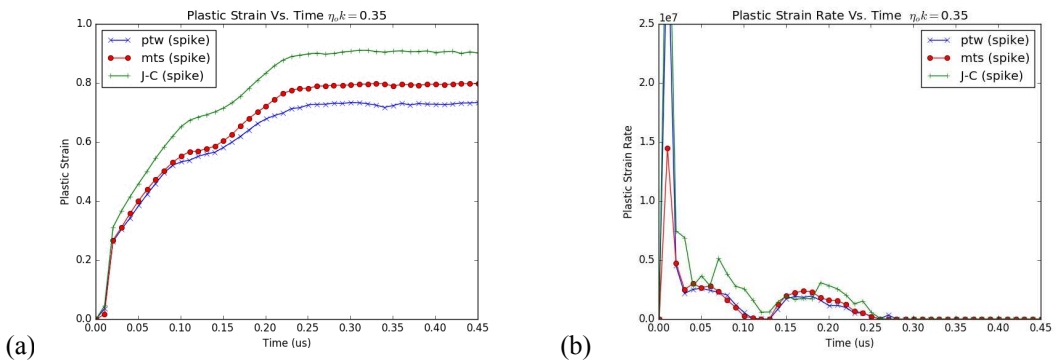

Fig. 6 Results for the RMI simulation for each model (a) plastic strain (b) plastic strain rate

3.2. Using Perturbation Growth Data to Calibrate the Johnson Cook Strength Model

To determine if the experimentally measured perturbation growth values might be used to calibrate the strength models in the intermediate regime, numerical sensitivity studies were performed with selected strength parameters in the Johnson Cook and PTW models. The PRDEF capability, was then used to observe the changes outside intermediate rates resulting from this tuning. Ideally, the available RMI data would be used to calibrate the "RAD" parameter in the PTW model since this parameter explicitly controls flow stress in the intermediate strain rate regime through a polynomial fit [16].

Unfortunately, this parameter does not sufficiently influence the computed perturbation growth because it changes saturation stress, not initial yield strength [13]. For the PTW strength model, in addition to confirming the lack of sensitivity in RAD for calibration to RMI data, the parameters YINF and SINF were also tested and it was demonstrated numerically that neither of these parameters is a good candidate for calibration to RMI spike height data.

For the empirically based Johnson-Cook model,

$$Y = Y\left(\varepsilon^p, \dot{\varepsilon}^p, T\right) = \left[A + B\left(\varepsilon^p\right)^n\right]\left[1 + C\ln\left(\dot{\varepsilon}\right)^p\right]\left[1 - \Theta_H^M\right] \quad (1)$$

$$\text{where, } \Theta_H = \left(\frac{T - T_{room}}{T_{melt} - T_{room}}\right)$$

simulations were conducted to investigate varying the initial yield stress using the "A" term and the strain hardening constant "C". Modifying the initial yield stress was effective in increasing strength in the intermediate range and improving spike growth estimates; however, this parameter appeared to be too blunt of a tool for tuning rate sensitivity and the computed peak velocities diverged from experiment. While not tested, lower rate predictions, such as Taylor anvil tests, would be expected to significantly diverge from experimental results since the "A" parameter influences stress across all strain rates. Alternatively, changing the "C" parameter is more targeted at affecting strength in the intermediate regime of interest. Changing "C" from its nominal value of $2.5\text{x}10^{-2}$ to a value calibrated to the RMI data of $2.5\text{x}10^{-1}$ resulted in the expected hardening behavior and brought the numerical estimates closer to the experimental value; however, velocity profile estimates again worsened.

Ultimately, a high strain rate version of the Johnson-Cook model [3] was implemented into the code in order to achieve higher yield stress values in the strain rate regime of interest:

$$Y = Y\left(\varepsilon^p, \dot{\varepsilon}^p, T\right) = \left[A + B\left(\varepsilon^p\right)^n\right]\left[1 + C\ln\left(\dot{\varepsilon}\right)^p + \boxed{C_2\ln\left(\dot{\varepsilon}^p\right)^{C_3}}\right]\left[1 - \Theta_H^M\right] \quad (2)$$

Using this high rate form of the Johnson-Cook model, and values for C_2 and C_3 calibrated to the spike height, resulted in significantly better agreement to experimentally determined spike growth and velocity profiles. The estimated spike growth of 164 μm from this high rate model was within 3% of the experimentally measured value and the peak velocity of 2.15 mm/μs matched the experimentally measured value in [8]. The sole difference between the standard Johnson-Cook model (equation 1) and high rate version (equation 2) is the expanded strain rate term (boxed) which allows for enhanced rate effect [3].

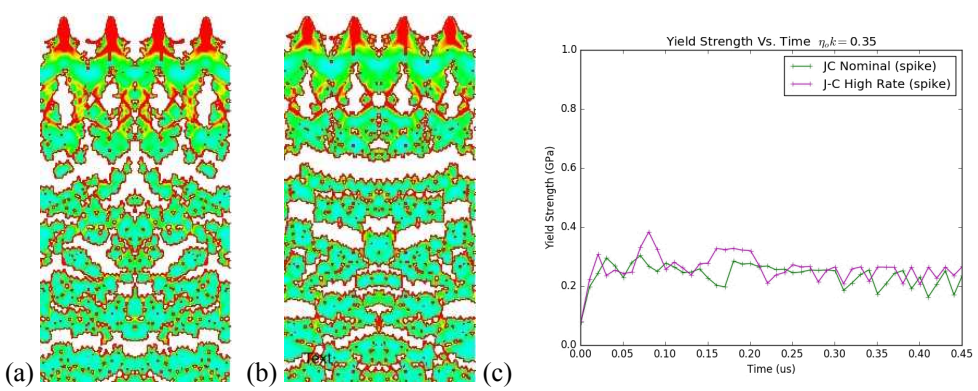

Fig. 7 Plastic Strain at 5 μs from shock arrival at the free surface (red = 1.0; green= 0.0) (a) Nominal Johnson-Cook (b) High-Rate Johnson-Cook (c) Yield Stress Comparison

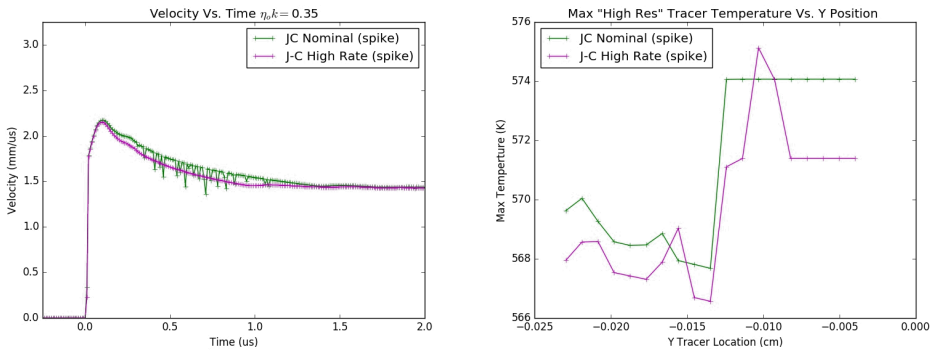

Fig. 8. Nominal Johnson-Cook Vs. High-Rate Johnson-Cook (a) Velocity (b) Maximum Temperature Under Spike

Figures 7-8 compare the nominal Johnson-Cook model with the high-rate Johnson-Cook model demonstrating that the parameters chosen for C_2 and C_3 produce subtle changes in the flow stress which can significantly affect spike height estimates. As shown in Figure 9, the additional term in the high rate Johnson-Cook model is effective at increasing flow stress in the intermediate strain rate regime of interest with modest changes to flow stress outside the targeted strain rate band.

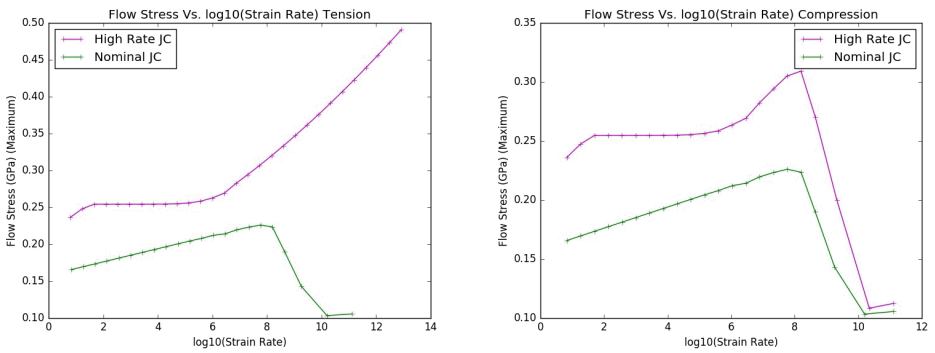

Fig. 9. PRDEF Simulations Comparing the Nominal Johnson-Cook Model with the High-Rate Johnson-Cook Model (a) Tension (b) Compression

4. Conclusions

The PTW, MTS and Johnson-Cook strength models were exercised against Richtmyer-Meshkov experimental results in the $\eta_0 k = .35$ configuration. The Johnson-Cook model generally under-estimates flow stress in this strain rate regime while PTW and MTS over-estimate flow stress at these rates. Additional effort is needed in tailoring strength models in the intermediate strain rate regime of 10^4 – 10^9 s^{-1} to take full advantage of available experimental data. Towards this end, existing PTW and Johnson-Cook parameters that might be calibrated to the RMI data were examined and a high rate version of the Johnson-Cook model was implemented into the code. The modified high rate Johnson-Cook model improved RMI estimates significantly using values for "C_2" and "C_3" that were calibrated to RMI spike growth data. The prescribed deformation capability in CTH was used to further examine the effects of this high rate Johnson-Cook model across a broader strain rate regime, from thermal activation to overdriven shock, and it was demonstrated that the proposed values only modestly affect strength outside the targeted intermediate regime. The simulations conducted suggest that with additional Richtmyer-Meshkov experimental data, the accuracy of material strength models in the intermediate strain rate regime can be further improved.

Acknowledgements

The authors would like to acknowledge the Joint DOE/DoD Munitions Program and the DOE Advanced Scientific Computing Physics and Engineering Program for supporting this work. Sandia is a multi-program Laboratory operated by Sandia Corporation, a Lockheed Martin Company, for the United States Department of Energy under contract DE-AC04-94-AL85000.

References

[1] Preston, D.L., Tonks, D.L., 2002. "Model of plastic deformation for extreme loading conditions", Journal of Applied Physics Volume 93, No. 1, 2003.
[2] Meyers, M.A., 1994. "Dynamic Behavior of Materials", John Wiley & Sons, New York, p. 323.
[3] Johnson, G.R., Holmquist, T.J., Anderson, C.E. and Nicholls, A.E., 2006. "Strain-rate effects for high-strain-rate computations", J. Phys. IV France 134 (2006) 391-396
[4] Follansbee, P.S., Kocks, U.F., 1988. "A Constitutive Description of the Deformation of Copper Based on the Use of the Mechanical Threshold Stress as an Internal State Variable", Acta metall. Vol. 36, No. 1, pp. 81-93, 1988
[5] Keinigs, R.K., 2000. "Strength Models for the Non-Expert: A Review of Six Constitutive Strength Relations and How They Compare at the Microscopic Level", Los Alamos National Laboratory report LA-UR-00-4500.
[6] Cranfield, T.R., Painter, J.W., et al, 2011. "PTW Mod 1 Implementation in FLAG", Los Alamos National Laboratory report LA-UR-05380.
[7] Banerjee, Biswajit, 2005. "An evaluation of plastic flow stress models for the simulation of high-temperature and high-strain-rate deformation of metals", arXiv:cond-mat/0512466
[8] W.T. Buttler, D.M. Oro, et al, 2012. "Unstable Richtmyer-Meshkov growth of solid and liquid metals in vacuum", J. Fluid Mech. (2012), vol. 703 pp. 60-84
[9] Wouchuk, J.G., 2001. "Growth rate of the linear Richtmyer-Meshkov instability when a shock is reflected", Physical Review E, Volume 63, 056303
[10] Richtmyer, R.D., 1960. "Taylor Instability in Shock Acceleration of Compressible Fluids", Communications on Pure and Applied Mathematics, Vol. XIII, 297-319 (1960)
[11] Meshkov, E.E., 1969. "Instability of the Interface of Two Gases Accelerated by a Shock Wave", Mekhankika Zhidkosti i Gaza, Vol. 4, No. 5, pp. 151-157, 1969
[12] Piriz, A.R., Lopez Cela, J.J., 2008. "Richtmyer-Meshkov instability in elastic-plastic media", Physical Review E 78, 056401 (2008)
[13] Prime, M.B., Vaughan, D.E., et al, 2013. "Using growth and arrest of Richtmyer-Meshkov instabilities and Lagrangian simulations to study high-rate material strength", Proceedings of the 18th International Conference on Shock Compression of Condensed Matter (APS-SCCM).
[14] Piriz, A.R., Lobez, J.J., Tahir, N.A., 2009. "Richtmyer-Meshkov instability as a tool for evaluating material strength under extreme conditions", Nuclear Instruments and Methods in Physics Research A 606 (2009) 139-141.
[15] McGlaun, J.M., Thompson, S.L., Elrick, M.G., 1990. "CTH: A Three-Dimensional Shock Wave Physics Code", International Journal of Impact Engineering Vol. 10, pp. 351-360, 1990
[16] Cranfield, T.R., Painter, J.W., et al, 2011. "PTW Mod 1 Implementation in FLAG", Los Alamos National Laboratory report LA-UR-05380.